Active and Passive Elec. Comp., 2003, Vol. 26(1), pp. 51–62

Taylor & Francis
Taylor & Francis Group

VOLTAGE-CONTROLLED SMALL SIGNAL ANALYSIS OF REAL SPACE TRANSFER TRANSISTOR

K. F. YARN[a,*] and J. Y. HWANG[b]

[a]*Department of Electrical Engineering, Far East College, Optoelectronic Semiconductor Center, Hsin-Shih, Tainan 744, Taiwan, Republic of China;* [b]*Department of Electrical Engineering, National Cheng-Kung University, Tainan 701, Taiwan, Republic of China*

(Received 7 November, 2002; In final form 17 November, 2002)

The research of determining the small signal equivalent circuit of the real space transfer (RST) transistor is investigated in this work. We propose a voltage-controlled mode model, called parameter extraction, to describe the performance of RST transistors at high frequency range. Besides, we also employ the value-determined model to simulate the microwave characteristics of RST and the theoretical and experimental results are compared. The influence of variables of RF performance is analyzed and theoretical results show that the cut-off frequency (f_T) is mainly affected by the leakage resistances and the dimension of metal contact, but the maximum available gain frequency, f_{max}, is dependent on contact resistances.

Keywords: Real space transfer (RST); Parameter extraction

1 INTRODUCTION

The real space transfer transistor is a three-terminal heterostructure device [1, 2] based on the real space transfer of hot electrons between two conducting layers and it is proposed by Kastalsky and Luryi [3]. There are two operation modes in RST transistor, one is negative resistance field effect transistor (NERFET) and the other is charge injection transistor (CHINT). The basis operation principle of CHINT is voltage-controlled real space carrier transfer in the channel. There are three terminals in CHINT, *i.e.*, source, drain and collector. When applying a heating voltage between drain and source, the average energy in quantum well is then enhanced and many hot electrons escaping over the internal barrier towards the collector. Then, a strong negative differential resistance (NDR) phenomenon is revealed in drain current.

In this report, a GaAs/InGaAs/AlGaAs RST transistor (RSTT) is grown by MOCVD. InGaAs is chosen as the channel layer due to its high electron mobility, AlGaAs as the internal barrier layer and GaAs as the top layer. A microwave measurement procedure for chip device in the test fixture and measurement technique of the extrinsic elements is then proposed. Accurate measurements at high frequency require calibration to compensate errors in the test system. In order to carry out the small signal circuit of RSTTs, the theoretical

* Corresponding author. E-mail: ymo86@yahoo.com.tw

ISSN 0882-7516 print; ISSN 0000-000X online
DOI: 10.1080/0882751000000000000

analysis is also proposed to fit the measured results. The influence of relative parameters is investigated by simulating the value-determined model.

2 THEORETICAL ANALYSIS

Before any device model can be used, all parameters in RSTTs must be determined by a process called parameter extraction. The parameter extraction method has been developed in many different ways which it depends on the operation mode of device. Generally, the catalog can be divided into two parts, *i.e.*, FET-like device and BJT-like device. Minasian [4] and other authors have discussed the direct extraction procedures for GaAs FETs [5–7], HEMTs [8] and BJTs. In this report, an extraction procedures is proposed to determine the equivalent small signal circuit of the RSTT.

2.1 Description of Small Signal Model

According to the operation mechanism of CHINT mode (*i.e.* modulate I_C by controlling V_{DS}), the voltage-controlled mode model is proposed. The small signal model of RSTT is shown in Figure 1. The equivalent circuit can be divided into two parts:

1. The intrinsic elements R_{DS}, R_{DC}, R_{CS}, C_{DS}, C_{DC}, C_{CS}, g_m, τ which are functions of the biasing conditions.
2. The extrinsic elements L_S, L_D, L_C, R_s, R_D and R_C which are independent of the biasing conditions.

Basically, the model consists of intrinsic components inside dashed box to model the physical layout of the real space transfer device and extrinsic components outside the dashed box

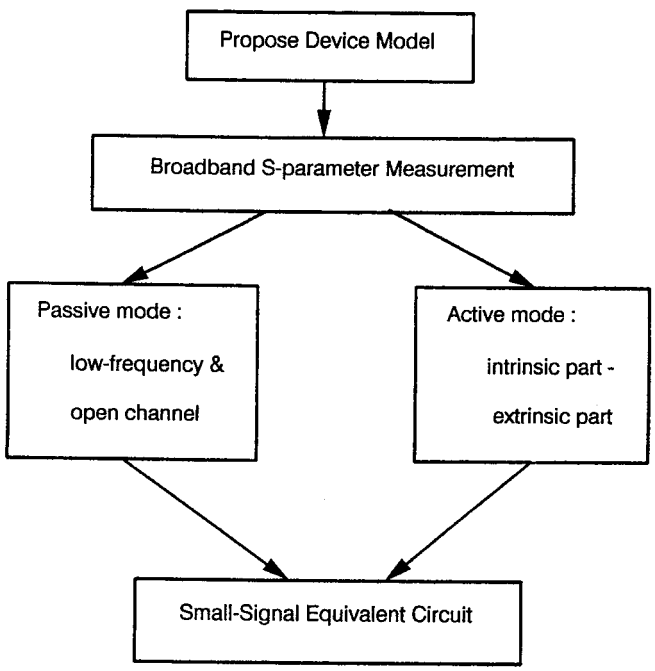

FIGURE 1 The flow chart for determining the small-signal equivalent of real space transfer transistors.

to describe parasitic effect. Because the transconductance g_m, cannot response the instantaneous change in drain voltage at microwave frequency, a transconductance delay time, τ, is included to provide phase shift in the collector current I_C. The flow chart of the main procedure fitting the measured results is shown in Figure 2.

2.2 Determination of the Parasitic Resistance and Inductances

The operation of real space transfer transistor can be considered as FET-like device. As Diament and Laviron have suggested [9], the S-parameter measurements at zero drain bias voltage can be used for the evaluation of device parasitic elements under the equivalent circuit shown in Figure 3 become simple. Therefore, the same condition can be available in the determination of the extrinsic elements in RSTTs, and the collector electrode behaves as a back-gate. The channel above the collector can be described by a distributed uniform R–C transmission line, leading to a simple analytical model which can be expected to be of good accuracy. The impedance Z-parameter matrix of the 2-port in the common source configuration is derived and given by

$$Z=\begin{bmatrix} R_S+R_C+j\omega(L_S+L_C)+\dfrac{\Gamma L}{j\omega C_C\tanh\Gamma L} & R_S+j\omega L_S+\dfrac{\Gamma L(\cosh\Gamma L-1)}{j\omega C_S\sinh\Gamma L} \\ R_S+j\omega L_S+\dfrac{\Gamma L(\cosh\Gamma L-1)}{j\omega C_C\sinh\Gamma L} & R_S+R_D+j\omega(L_S+LD)+\dfrac{2\Gamma L(\cosh\Gamma L-1)}{j\omega C_C\sinh\Gamma L} \end{bmatrix}$$

where $\Gamma L=(R_{\mathrm{ch}}C_c)$ is the propagation constant of the R–C transmission line, L is the channel length, C_C is the geometric depletion layer capacitance and R_{ch} is the channel resistance. Using low frequency and open channel condition, the Z-parameter matrix is further simplified. Assume the condition to be met, Z-parameter matrix can be reduced to:

$$Z=\begin{bmatrix} R_S+R_C+\dfrac{1}{3}R_{\mathrm{ch}}+j\omega(L_S+L_C) & R_S+\dfrac{1}{2}R_{\mathrm{ch}}+j\omega L_S \\ R_S+\dfrac{1}{2}R_{\mathrm{ch}}+j\omega L_S & R_S+R_D+R_{\mathrm{ch}}+j\omega(L_S+L_D) \end{bmatrix}$$

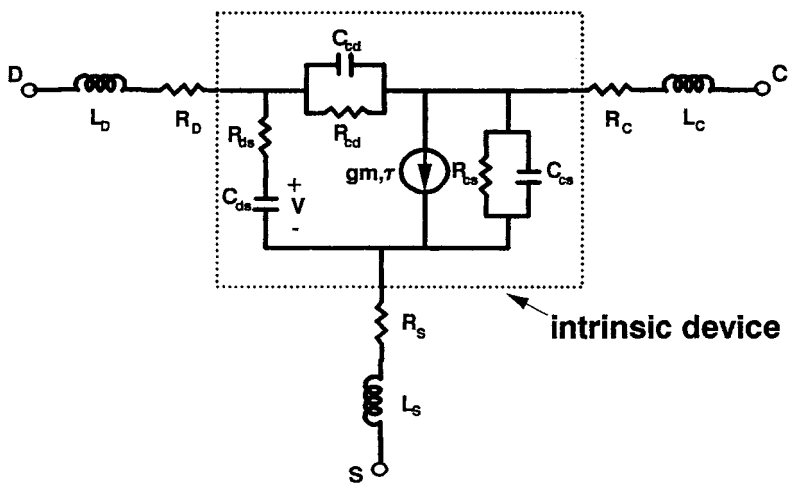

FIGURE 2 Small-signal equivalent circuit of a real space transfer transistor.

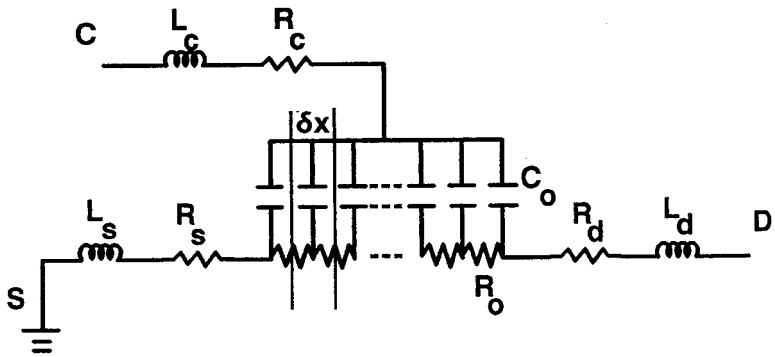

FIGURE 3 Equivalent circuit model under low frequency and open channel condition.

The matrix conversion from S parameters measured in this condition to Z-parameters is required in the procedure, where $[Z] = [Z_0]([I] + [S])([I] - [S])^{-1}$.

The imaginary part of Z-parameters versus frequency characteristics is shown in Figure 4. Then, L_S, L_D and L_C are got from the imaginary part of Z_{12}, Z_{22} and Z_{11}. Besides, the real part of Z-parameters provide three relations between the four unknown R_S, R_D, R_C and R_{ch}. Therefore, an additional relation is needed to separate the four unknowns. Usually R_S and R_D can be obtained readily from DC measurement or other developed methods [10–12].

As a result, the series parasitic elements R_S, R_D, R_C, L_S, L_D and L_C can be provided by performing the S-parameter measurement under zero drain and forward collector bias voltage. Under such measurement condition, the value of extrinsic elements of RSTTs with channel length 2 μm is shown in Table I.

2.3 Determination of the Intrinsic Elements

Once the extrinsic parameters are known, the intrinsic parameters can be extracted with following steps as shown in Figure 5.

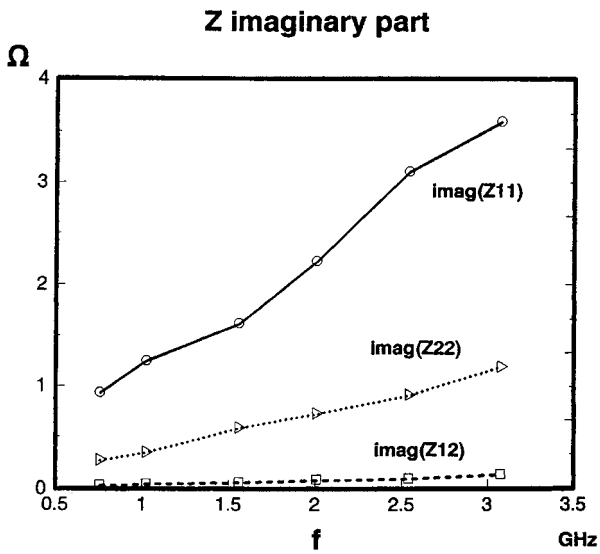

FIGURE 4 The Z-parameters' imaginary part *vs.* frequency under forward collector bias voltage and zero drain bias voltage.

TABLE I Extrinsic Elements of RSTTs.

Extrinsic parameters	*Value*
R_S	8.45 Ω
R_D	19.55 Ω
R_C	1.43 Ω
L_S	0.037 nH
L_D	0.3 nH
L_C	1.13 nH

1. Measurements of the S-parameters at normal operating collector and drain bias voltages in the 130 MHz to 10 GHz frequency range.
2. Transformation of the S-parameter matrix to Z-parameter matrix and subtraction of R_S, R_D, R_C, L_S, L_D and L_C that are in series.
3. Transformation of Z-parameter matrix to Y-parameter matrix corresponding to the derived matrix. Therefore, the determination of the intrinsic admittance (Y) matrix can be carried out using some simple matrix manipulations. Since the intrinsic device model shown in Figure 6 exhibits a π topology, it is convenient to use the Y-parameters to characterize its electrical properties. Using the circuit analysis of 2-port network above, y parameter matrix can be given

$$\begin{bmatrix} I_1 \\ I_2 \end{bmatrix} = \begin{bmatrix} y_{11} & y_{12} \\ y_{21} & y_{22} \end{bmatrix} \begin{bmatrix} V_1 \\ V_2 \end{bmatrix} = \begin{bmatrix} \dfrac{V_1}{R_{\mathrm{DS}} + 1/(j\omega C_{\mathrm{DS}})} + \dfrac{V_1 - V_2}{R_{\mathrm{DC}} \| C_{\mathrm{DC}}} \\ \dfrac{V_2}{R_{\mathrm{CS}} \| C_{\mathrm{CS}}} + \dfrac{V_2 - V_1}{R_{\mathrm{DC}} \| C_{\mathrm{DC}}} + g_m \exp(-j\omega\tau) V \end{bmatrix}$$

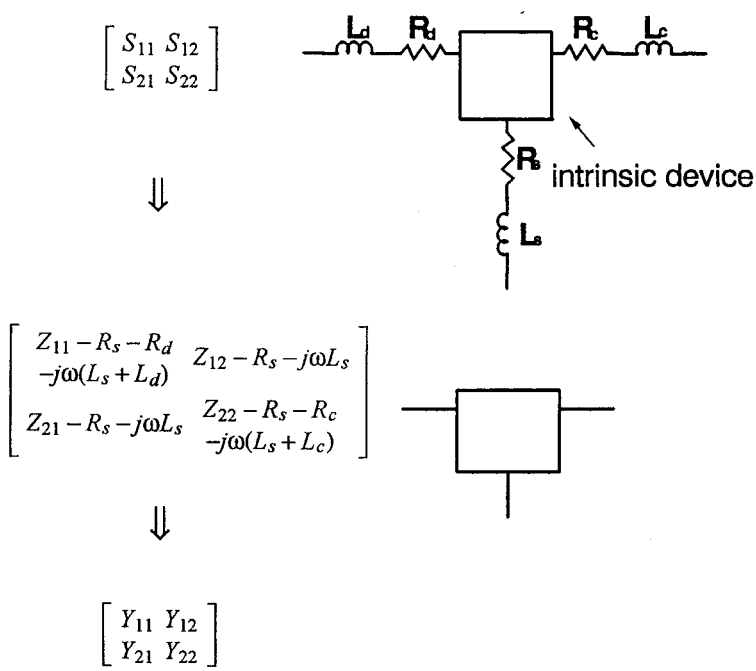

FIGURE 5 The procedure for extracting the intrinsic elements.

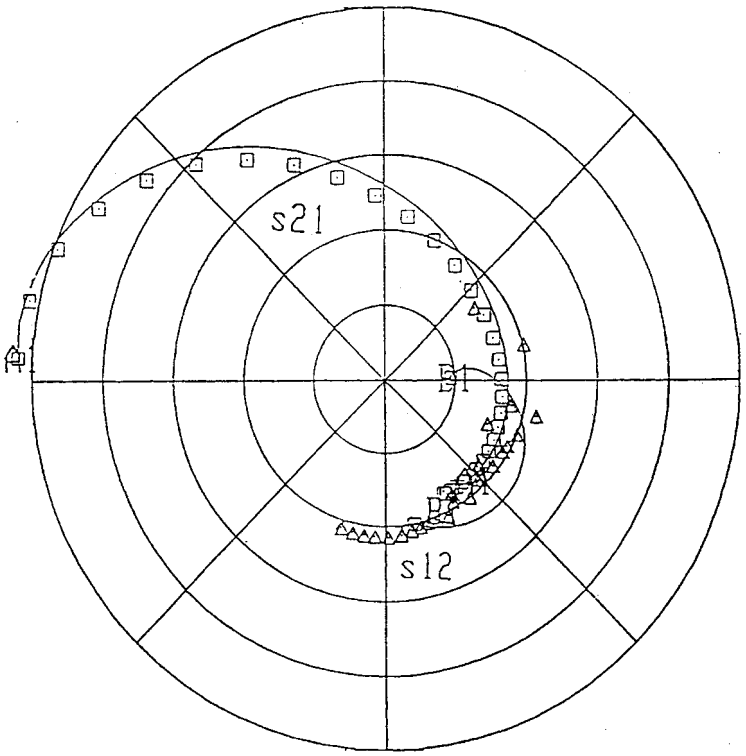

FIGURE 6 The measured and simulated S_{21}, S_{12} from 130 MHz to 10 GHz.

where

$$V = \frac{V_1}{R_{DS} + 1/(j\omega C_{DS})} \frac{1}{j\omega C_{DS}} = \frac{V_1}{1 + j\omega C_{DS} R_{DS}}$$

Assume $\omega^2 C_{DS}^2 R_{DS}^2 \ll 1$, then get:

$$y_{11} = \left(\frac{1}{R_{DC}} + \omega^2 R_{DS} C_{DS}^2\right) + j\omega(C_{DS} + C_{DC})$$

$$y_{12} = -\frac{1}{R_{DC}} - j\omega C_{DC}$$

$$y_{21} = g_m(1 - \omega^2 \tau C_{DS} R_{DS}) - \frac{1}{R_{DC}} - j\omega(C_{DC} + g_m(\tau + C_{DS} R_{DS}))$$

$$y_{22} = \left(\frac{1}{R_{CS}} + \frac{1}{R_{DC}}\right) + j\omega(C_{CS} + C_{DC})$$

Expressions above show that the intrinsic small signal elements can be deduced from the Y-parameters as follows:

R_{DC} and C_{DC} are from the real and imaginary part of y_{12}, respectively. Then, R_{DS}, C_{DS}, R_{CS} and C_{CS} can be calculated from y_{11} and y_{22} after subtraction of R_{DC} and C_{DC}. Next, g_m and τ can be got from y_{21} by several mathematical manipulations. Therefore, the intrinsic elements R_{DS}, R_{DC}, R_{CS}, C_{DS}, C_{DC}, C_{CS}, g_m and τ can be easily extracted from the measured results in Figure 6. The f_T and f_{max} of the studied RSTT is near 2 GHz, so the simulated frequency is chosen from 130 MHz to 1.52 GHz. The fitting results are shown in Table II. We get

TABLE II Intrinsic Elements of RSTTs.

	Intrinsic parameters							
	R_{DS} (Ω)	R_{DC} (Ω)	R_{CS} (Ω)	C_{DS} (fF)	C_{DC} (fF)	C_{CS} (fF)	g_m (mS)	τ (ps)
130 MHz	−193	193.2	129.1	261	527	242	43.1	9.91
622 MHz	−199.5	215.7	123.5	310	586	302	38	8.95
1.024 GHz	−210	287.1	149.1	190	559	345	34.2	10.03
1.52 GHz	−203.7	221.6	141	381	643	341	42	11.25
	−201.3	236.9	135	287	581	305	39.3	10.3

$C_{\mathrm{DS}} = 287$ fF, $R_{\mathrm{DS}} = -201.3\ \Omega$. For $f = 1$ GHz, $\omega^2 C_{\mathrm{DS}}^2 R_{\mathrm{DS}}^2 = 0.0033 \ll 1$, the assumption to obtain the simplified y-parameter matrix is reasonable.

3 RESULTS AND DISCUSSION

The small signal equivalent circuit of RSTTs has been extracted from the measured S-parameters. In order to check up our fitting procedure, the value-determined small signal equivalent circuit is employed to simulate its high frequency characteristics by using the HP microwave design system (MDS) software [13] and the S-parameters computed from the equivalent circuit are compared with the measured S-parameters. Figure 6 shows the measured and simulated S_{21} and S_{12} together. Both of the measured and simulated S_{21} are very close and their tendencies are the same. Besides, the measured and simulated S_{12} are not very matched, but that can be accepted. Figure 7 shows the results of the comparison

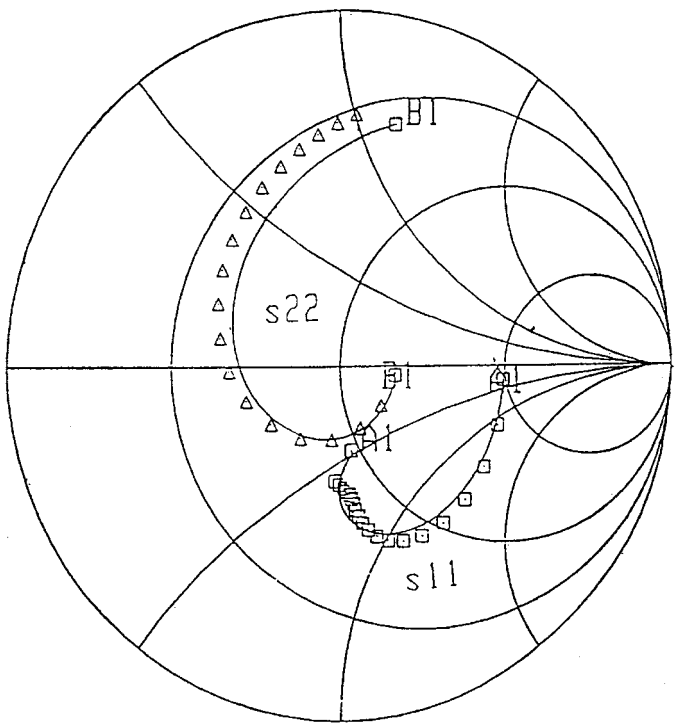

FIGURE 7 The measured and simulated S_{11}, S_{22} from 130 MHz to 10 GHz.

of S_{11} and S_{22}. The simulated curves are in quite good agreement with the measured curves from 130 MHz to 10 GHz. Figure 8 shows the measured and simulated f_T and f_{max}. The track of curves is not very fitting beyond 1 GHz because the fitting points are only chosen from 130 MHz to 1.52 GHz. The influence of the model components on frequency response also takes a great deal of interest to us. Figure 9 displays frequency characteristics as functions of R_{CS}, R_{DC}. All of them show various degree of effects on f_T and f_{max}, especially, for R_{DC}. The decrease of R_{DC} will result in the decrease of f_{max}. R_{DC} and R_{DS} are also influential on f_T. If the leakage resistances between collector-to-drain and collector-to-source increase, the higher f_T and f_{max} can be expected. Therefore, those leakage resistances will be increased with: (a) the decrease of collector, drain and source contact area, (b) the increase of barrier thickness and (c) high quality undoped barrier layer. In addition, the less negative resistance induced in the channel will obtain the higher f_T and f_{max} which can be seen in Figure 10.

Figure 11 shows R_D, R_S versus frequency characteristics. On the whole, f_T is independent of those contact resistances and f_{max} decreases with increasing the contact resistances. So, the lower metal contact ohmic resistances are required for power RST devices. In addition, when R_D is reduced to 2.5 Ω, the unstable phenomenon is found and f_{max}, is determined by maximum stable gain (MSG). Figure 12 shows the dependence of C_{DC}, C_{DS} on frequency characteristics. The f_T and f_{max} increase with decreasing the C_{DC} strongly. From the relation of $C = \varepsilon A/d$, it is easy to know that when reducing the collector and drain contact dimension or increasing the thickness of barrier will get lower C_{DC} to obtain higher f_T and f_{max}. The condition is much the same as the leakage resistances. As shown in Figure 12, C_{DS} also influences f_T profoundly. If the depth of drain and source sintering contact is lower or the undoped GaAs layer under cap layer is removed, the smaller capacitance between source and drain can be achieved.

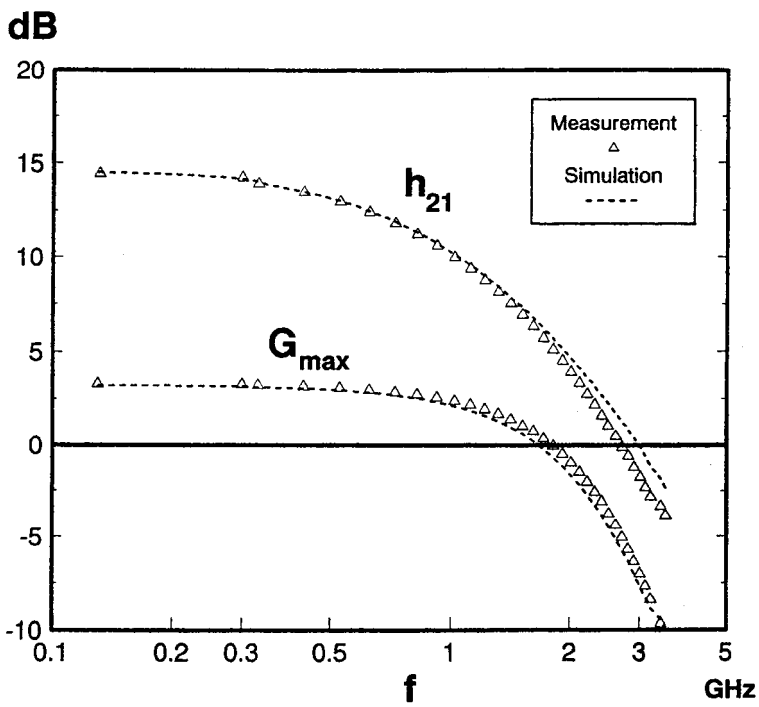

FIGURE 8 Comparison between the measured and calculated f_T, f_{max}.

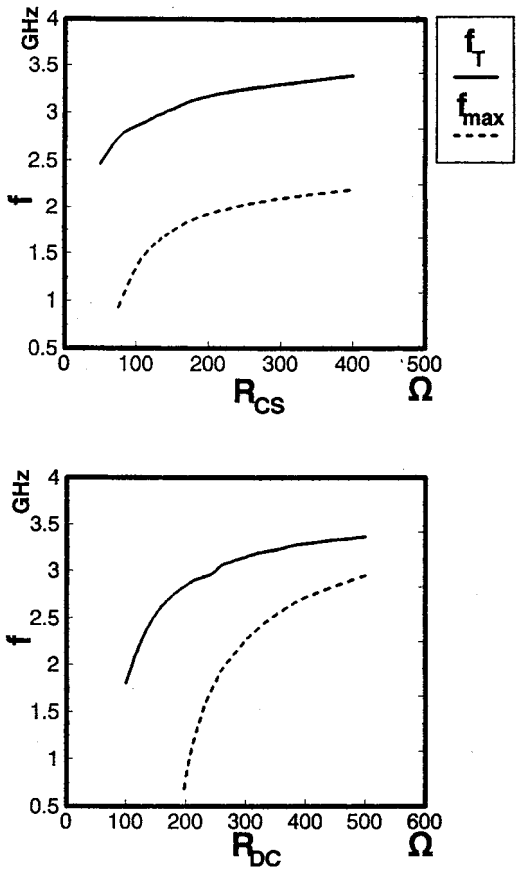

FIGURE 9 The dependence of R_{DC}, R_{CS} on frequency characteristics.

In our investigation, the shorter delay time will increase f_T and f_{max}. Essentially, the delay time τ consists of two parts: (a) the time required to establish an electron temperature in the channel and (b) the flight time of hot electrons across the barrier layer. Therefore, shorter channel length and thinner barrier layer are of great advantage to τ. However, the tendency of barrier thickness on delay time is contrary to the results we get from the leakage resistances and capacitances. Thus, the trade-off between τ and the leakage resistances (or capacitances) can be made by modulating the barrier thickness. Therefore, the improved parameters can be accomplished by several methods as follows:

1. The reduction of collector contact area can obtain high leakage resistances and capacitances.
2. The decrease of the thickness of the evaporated contacts will decrease the parasitic inductances.
3. Lower ohmic resistances.

As those improved parameters listed in Table III, the f_T and f_{max} can be 42.51 GHz and 47 GHz, respectively (f_{max} is obtained by the maximum stable gain (MSG) due to $K < 1$). In addition, no significant phenomenon [11], the magnitude of S_{11} is larger than unity, is presented because the contact resistances of our devices is rather large to suppress the above behavior.

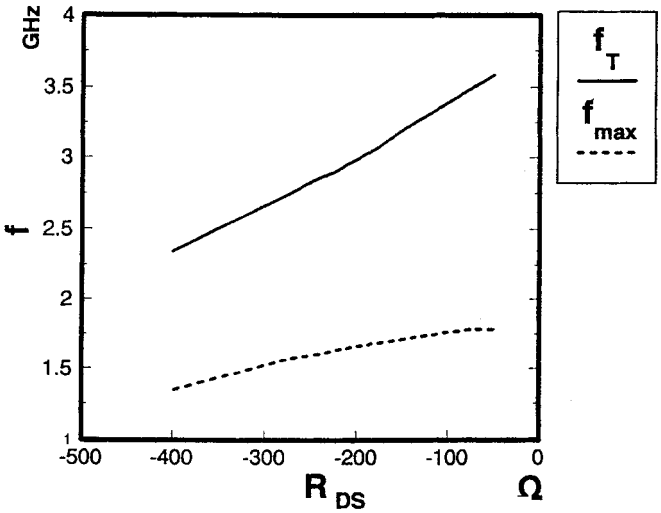

FIGURE 10 The dependence of R_{DS} on frequency characteristics.

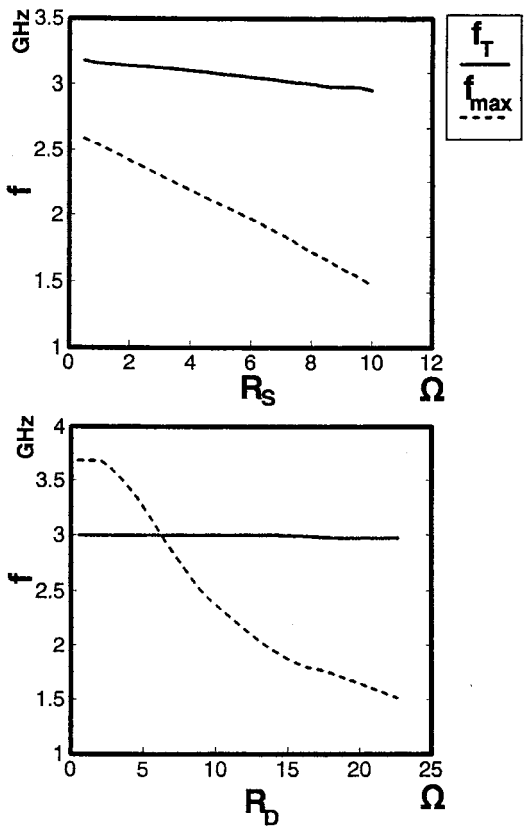

FIGURE 11 The dependence of R_D, R_S on frequency characteristics.

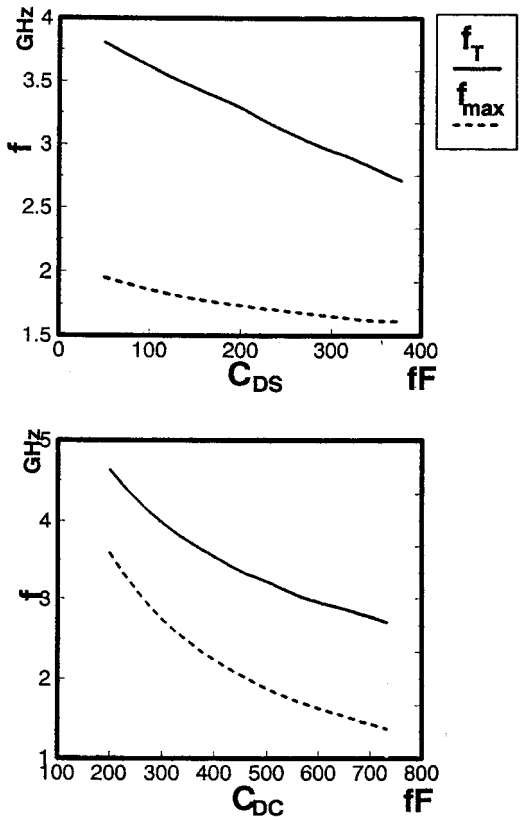

FIGURE 12 The dependence of C_{DC}, C_{DS} on frequency characteristics.

TABLE III The Improved Parameters.

Ohmic resistance	$R_C = 0.5\,\Omega$;	$R_S = 0.5\,\Omega$;	$R_D = 0.5\,\Omega$
Capacitance	$C_{CS} = 0.1$ pF;	$C_{DC} = 0.1$ pF;	$C_{DS} = 0.052$ pF
Leakage resistance	$R_{DS} = -100\,\Omega$;	$R_{CS} = 200\,\Omega$;	$R_{DC} = 236\,\Omega$
Parasitic inductance	$L_C = 0.25$ nH;	$L_S = 0.25$ nH;	$L_D = 0.25$ nH
f_T	42.51 GHz		
f_{max}	46.25 GHz		

4 CONCLUSIONS

We have proposed a direct method to determine the small signal equivalent circuit components of RSTTs in CHINT mode. Although the extrinsic elements are determined at relatively low frequency, quite good agreement between theoretical and experimental *S*-parameters can be achieved near 10 GHz. That provides the validity of our approach. Then, intrinsic elements are easy to determine by a few simple matrix manipulations after the determination of the extrinsic elements. From the investigation of frequency characteristics of RSTTs, the improvements on device performance are as follows:

1. Reduce the dimension of metal contacts to increase the leakage resistances and reduce the capacitance in barrier.

2. The increase of barrier thickness will decrease the capacitances and increase the leakage resistances, but that disagrees with the improvement of τ.
3. The decrease of ohmic contact resistance by the non-alloyed epitaxial contact or shallow ohmic contact can improve the power dissipation for power RST devices.

References

[1] Hess, K., Morkoc, H., Shichijo, H. and Streetman, B. G. (1979). *Appl. Phys. Lett.*, **35**, 469.
[2] Kastalsky, A. and Luryi, S. (1983). *IEEE Electron. Dev. Lett.*, **EDL-4**, 334.
[3] Luryi, S., Kastalsky, A., Gossard, A. C. and Hendel, R. H. (1984). *IEEE Trans. Electron. Dev.*, **31**, 832.
[4] Minasian, R. A. (1977). *Electron. Lett.*, **13**, 549.
[5] Arnold, E., Golio, M., Miller, M. and Beckwith, B. (1990). *IEEE Microwave Theory Technol. Symp. Digest*, 359.
[6] Wurtz, L. T. (1994). *IEEE Instru. and Measur.*, **43**, 655.
[7] Vogel, R. (1987). *Proc. 17th European Microwave Conference*, 616.
[8] Hughes, B. and Tasker, P. J. (1989). *IEEE Trans. Electron. Dev.*, **36**, 2267.
[9] Diamant, F. and Laviron, M. (1982). *Proc. 12th European Microwave Conference*, 451.
[10] Fukui, H. (1979). *Bell Syst. Tech. J.*, **58**, 771.
[11] Lee, K. W., Lee, K., Shur, M. S., Vu, T. T., Roberts, C. T. and Helix, M. J. (1986). *IEEE Electron. Dev.*, **7**, 75.
[12] HP Company, Discovering the system: Building and analyzing circuits, HP 85150B Microwave Design System User's Guide.